Accurate Estimation of Harmonic and Non-harmonic Components Using the NLT and Vector Fitting

C.E. Román-López, E.S. Bañuelos-Cabral, J.A. Gutiérrez-Robles, V.A. Galván-Sánchez and C.A López de Alba.

***Abstract*—Analysis and estimation of harmonic and non-harmonic content in electrical power systems play an important role in standards compliance and system safety. This paper presents a methodology for accurately estimating harmonic and non-harmonic components (subharmonics, interharmonics, supraharmonics, and/or exponentials) using the Numerical Laplace Transform (NLT) and Vector Fitting (VF). The proposed methodology involves adding a magnitude and phase of a known harmonic base to the signals being studied to ensure that VF converges to this harmonic base. Subsequently, in the parameter calculation stage, the added components are subtracted to obtain the desired harmonic estimation of the signals. Non-harmonic components are those to which VF converges but are not part of the aggregated base. The proposed methodology is demonstrated in two test cases: 1) synthetic signals containing both harmonic and non-harmonic components to which successfully have been estimated 1, 50, and 1000 harmonics and 2) the simulation of an induction motor controller. Results show that this methodology can fully decompose a signal into harmonic and non-harmonic components with a high degree of accuracy.**

***Keywords*: Numerical Laplace Transform, Non-harmonic components, Harmonic components, Vector Fitting.**

I. Introduction

ALONG with its impact on power quality in modern electrical power systems, the associated technologies with power electronics, renewable energy, and energy efficiency are becoming increasingly relevant. Due to its implementation, power grid waveforms such as voltages or currents may present distortions caused by harmonic and non-harmonic components (subharmonics, interharmonics, supraharmonics, exponentials, and/or DC offset). These distortions can negatively affect several aspects of the electrical system, including aging of insulating materials, capacitor failures in electronic devices, interference in communications, and energy measurement errors, among others [1-4].

For power quality studies, the Discrete Fourier Transform (DFT) is a widely used technique implemented through the Fast Fourier Transform (FFT). However, it has some limitations, such as the picket-fence effect, spectral leakage, and sensitivity to frequency deviations.

C.E. Román-López, E.S. Bañuelos-Cabral, J.A. Gutiérrez-Robles, V.A. Galván-Sánchez and C.A López de Alba are with the University of Guadalajara, Mexico.
(e-mail of corresponding author: eduardo.banuelos@academicos.udg.mx).

Paper submitted to the International Conference on Power Systems Transients (IPST2025) in Guadalajara, Mexico, June 8-12, 2025.

Several alternatives have been proposed, such as the Prony method, which, although it offers high resolution, is computationally inefficient and sensitive to noise, or the Matrix Pencil method (MP) [5] which has shown acceptable results in the presence of noise.

Hence, improving methodologies for analysis and estimation of harmonic and non-harmonic components is crucial for ensuring effective control and mitigation of power quality parameters [6].

The Numerical Laplace Transform (NLT) and the Vector Fitting (VF) method [7] have already been used to determinate some signal parameters, e.g., electromechanical oscillation modes [8]. More recently, the Extended Vector Fitting (EVF) method was presented to estimate subharmonics, harmonics, interharmonics, and supraharmonics from electrical system signals [9]. EVF allows approximating a function in the frequency domain with known and unknown poles, where the known poles correspond to harmonics and the unknown poles to non-harmonic components.

This paper presents an accurate methodology for simultaneously estimating the harmonic and non-harmonic content of a signal or group of signals using the NLT and the conventional VF. This approach requires no modifications to the VF method. The proposed methodology is based on the addition of a known harmonic base to the signals under study. The effect of this addition is then canceled through a subtraction process in the Frequency Domain (FD), thus forcing the VF to converge to a desired harmonic basis. Moreover, an iterative refinement for improving the estimation of components is presented. The proposed methodology is validated using (1) synthetic test signals and (2) the simulation of an induction motor controlled by a space vector pulse width modulation (SV-PWM) technique in Simulink.

II. Estimation of Harmonic and Non-harmonic Components using NLT and VF: Proposed Methodology

The NLT is used to obtain the images in Frequency Domain (FD) from the signals in Time Domain (TD) for its later rational approximation using VF. An overview of NLT theory is presented in [9-12].

A. Vector Fitting Iteration

The goal of VF is to approximate a data set through a model based on rational function in pole-residue form (1) with a finite number of poles N, typically defined by the user [7]. These data may consist of measured or calculated frequency-domain samples, expressed as $(s_k, \breve{h}_k)$ with $\breve{h}_k = \breve{h}(s_k)$ for $s_k = \mathrm{j}\omega_k,\ k = 1, \ldots, K$.

$$\breve{h}_k \cong h(s;\mathbf{x}) = \sum_{n=1}^{N} \frac{r_n}{s-p_n} + r_0. \tag{1}$$

In (1), $\mathbf{x}$ represents a vector with poles, residues, and constant term (p_n, r_n, r_0) used for the rational approximation. VF iteratively refines the position of the initial poles, (p_n^v); where the number of iterations, v, is also typically defined by the user. It then calculates the residues and the constant term in one step. For multiple scalar functions $\breve{h}_i(s_k), i = 1, \dots M$ and assuming they share the same poles, these responses can be stacked in a column vector as: $\breve{\mathbf{h}}_k$. Through VF, it is possible to obtain a set of common poles (2) for the constructed column vector: $(s_k, \breve{\mathbf{h}}_k)$ for $k = 1, \dots, K$.

$$\breve{\mathbf{h}}_k \cong \mathbf{h}(s;\mathbf{x}) = \sum_{n=1}^{N} \frac{\mathbf{r}_n}{s-p_n} + \mathbf{r}_0. \tag{2}$$

B. Proposed Methodology

Now, consider a power electrical signal defined by

$$f(t) \cong \psi + \left[\sum_{n=1}^{N_h} A_n \cos(n\omega_0 t + \theta_n)\right] + \left[\sum_{m=1}^{N_c} A_m\, e^{\alpha_m t}\cos(\omega_m t + \theta_m) + \sum_{l=1}^{N_r} A_l e^{\alpha_l t}\right]. \tag{3}$$

The first bracket in equation (3) represents the harmonic components, with a fundamental frequency of $\omega_0 = 2\pi f_0$ and where A_n is the amplitude and θ_n is the phase for the *n*th component. Additionally, ψ in (3) represents the DC offset. The second bracket in equation (3) considers the non-harmonic components. These have a frequency of $\omega_m = 2\pi f_m$ and a damping factor of α_m, where A_m is the amplitude and θ_m is the phase for the *m*th component. It also includes N_r exponential functions of amplitude A_l with a damping factor of α_l.

The Laplace Transform of (3) can be expressed as

$$F(s) = \left[\frac{\psi}{s}\right] + \left[\frac{1}{2}\sum_{n=1}^{N_h}\left(\frac{A_n e^{j\theta_n}}{s-jn\omega_0} + \frac{A_n e^{-j\theta_n}}{s+jn\omega_0}\right)\right] + \left[\frac{1}{2}\sum_{m=1}^{N_c}\left(\frac{A_m e^{j\theta_m}}{s-\alpha_m-j\omega_m} + \frac{A_m e^{-j\theta_m}}{s-\alpha_m+j\omega_m}\right) + \sum_{l=1}^{N_r}\frac{A_l}{s-\alpha_l}\right]. \tag{4}$$

Equation (4) rewritten according to equation (1):

$$F(s) = \left[\frac{r_1}{s}\right] + \left[\sum_{n=1}^{N_h}\left(\frac{\gamma_n + j\eta_n}{s-jn\omega_o} + \frac{\gamma_n - j\eta_n}{s+jn\omega_o}\right)\right] + \left[\sum_{m=1}^{N_c}\left(\frac{\gamma_m + j\eta_m}{s-\delta_m-j\beta_m} + \frac{\gamma_m - j\eta_m}{s-\delta_m+j\beta_m}\right) + \sum_{l=1}^{N_r}\frac{r_l}{s-p_l}\right]. \tag{5}$$

Equation (5) represents the rational approximation of VF for the signal defined in (3). The challenge here is to find and match each parameter of (3) and (5), considering (4), and to ensure VF convergence.

To overcome this challenge, the Extended Vector Fitting (EVF) method, presented in [9], calculates a rational function by assuming that some poles are known (harmonic components) and others are unknown (non-harmonic components), resulting in the following expression:

$$\breve{h}_k \cong h(s;\boldsymbol{x}) = \sum_{n=1}^{N_1} \frac{\breve{r}_n}{s-\breve{p}_n} + \sum_{n=1}^{N_2} \frac{r_n}{s-p_n} + r_0. \tag{6}$$

where $\breve{r}_n$ are the residues of the known poles $\breve{p}_n$ and r_n are the residues of the unknown poles, p_n. However, the numerical implementation of EVF requires modifying the VF algorithm.

The methodology proposed in this work consists of adding the magnitude and phase of a known harmonic base to the signals under study to ensure that VF converges to said harmonic base. During the parameter calculation stage, the added components are subsequently subtracted, yielding the desired harmonic estimation of the signals.

A full-wave rectified sinusoidal signal with a frequency of $f_0/2$ and amplitude B serves as the known harmonic base:

$$f_b(t) = B_o + \sum_{n=1}^{N_h} B_n \cos(n\omega_o t + \theta_n)$$
$$\text{With } B_n = \left|\frac{4B}{\pi(1-(2n)^2)}\right|,\ B_0 = \frac{2B}{\pi} \text{ and } \theta_n = \pi. \tag{7}$$

This harmonic base contains all harmonics of the fundamental frequency f_0 and their phases of π for all components. The behavior of $f_b(t)$ for $f_0 = 50$ Hz and $B = 1$ is shown in Fig.1a. Figs. 1b and 1c display the amplitude spectrum and phase spectrum, respectively.

The Laplace Transform of the sum of (3) and (7) is

$$\hat{F}(s) = \left[\frac{\psi + B_o}{s}\right] + \left[\frac{1}{2}\sum_{n=1}^{N_h}\left(\frac{A_n e^{j\theta_n} + B_n e^{j\theta_n}}{s-jn\omega_0} + \frac{A_n e^{-j\theta_n} + B_n e^{-j\theta_n}}{s+jn\omega_0}\right)\right] + \left[\frac{1}{2}\sum_{m=1}^{N_c}\left(\frac{A_m e^{j\theta_m}}{s-\alpha_m-j\omega_m} + \frac{A_m e^{-j\theta_m}}{s-\alpha_m+j\omega_m}\right) + \sum_{l=1}^{N_r}\frac{A_l}{s-\alpha_l}\right]. \tag{8}$$

The added harmonic base (7) allows VF to numerically converge to the harmonics. Finally, the signal parameters are calculated from the rational approximation of VF and subtracting the added basis considering (5) and (8):

$$\begin{aligned} \psi &= r_1 - B_o \\ A_n e^{j\theta_n} &= 2(\gamma_n + j\eta_n) - B_n e^{j\theta_n} \\ A_m e^{j\theta_m} &= 2(\gamma_m + j\eta_m) \\ \alpha_m &= \delta_m \\ \omega_m &= \beta_m. \end{aligned} \tag{9}$$

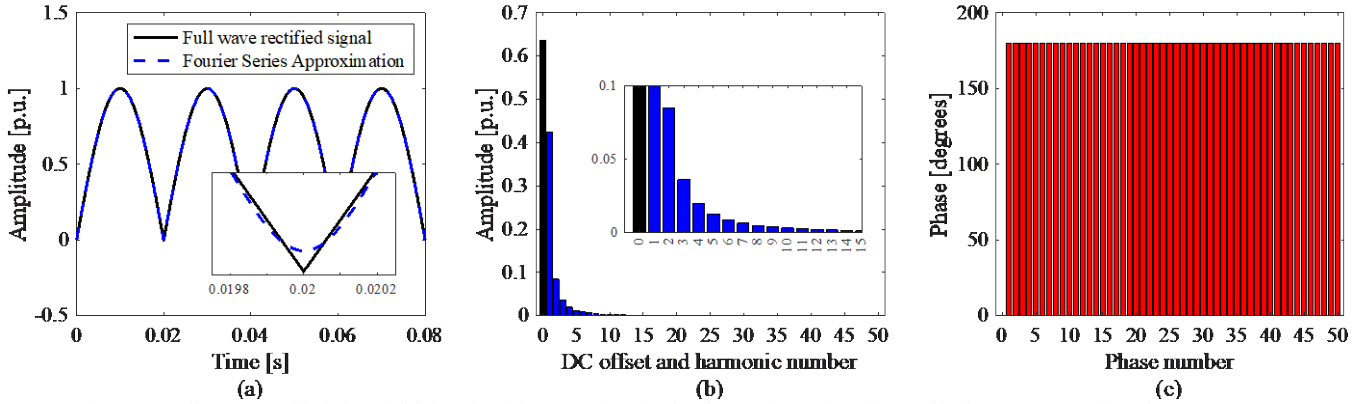

Fig.1. (a) Full-wave rectified sinusoidal signal and its approximation by the Fourier series, (b) Amplitude spectrum and (c) Phase spectrum.

An important advantage of this methodology is that by using the conventional VF algorithm, it is possible to identify the harmonic and non-harmonic components of multiple signals using common poles (2). It is possible to calculate the harmonic content of multiple signals accurately.

C. *Implementation and iterative refinement*

The implementation of this methodology together with an iterative refinement could be summarized as follows (Fig.2):

1) Calculate the FD representation of the signal or group of signals using the NLT. Experience has shown the NLT with the trapezoidal integration rule to be more accurate [10-11].
2) Define the number of harmonics to be calculated for the signal set, N_h. This value also determines the number of synthetic harmonics (7) to be added to the signal set. The frequency of the highest order harmonic defines the cut-off frequency for the data used in the rational approximation.
3) Transform the components calculated in Equation (7) to the FD and add them to the NLT data. While the signals under study may or may not present all the harmonics of the aggregated base, this aggregated base allows forcing VF convergence.
4) Define the number of poles according to the non-harmonic components to be calculated from the signal group, $N_n = 2N_c + N_r$. The total order for the approximation will be the sum: $N = 2N_h + N_n + 1$.
5) Use the conventional VF algorithm to calculate the rational approximation of the data. At this stage, it is possible to implement *an iterative refinement* to obtain better accuracy. This refinement consists on: 1) At each iteration it is possible to round each pole calculated by VF with respect to the added basis, since these components are known to be present in the data, and 2) The order N_n can be varied in each iteration, since it is not known how many are presented in the signals.
6) Use the relative dominant pole measurement (RDPM) [8] to eliminate those poles that have no impact on the rational approximation.
7) Finally, derive the signal parameters from the rational approximation of VF according to (9).

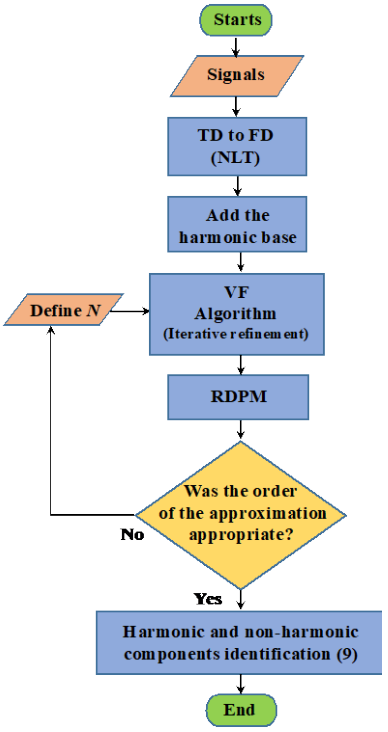

Fig.2. Flowchart of the proposed methodology.

III. Test Cases

A. *Synthetic test signals*

The proposed methodology is first evaluated using the following set of synthetic signals:

$$\begin{aligned} f_1(t) &= 1.1 + triang(2\pi f_0 t) + 0.2e^{-31t} \\ &+ 0.3e^{-30t}\cos(2\pi 120t) + 0.2\cos(2\pi 1275t) \\ f_2(t) &= 0.95 + triang(2\pi f_0 t + 120°) + 0.25e^{-30t} \\ &+ 0.35e^{-28t}\cos(2\pi 120t) + 0.2\cos(2\pi 1275t + 120°) \\ f_3(t) &= 1.2 + triang(2\pi f_0 t - 120°) + 0.28e^{-30t} \\ &+ 0.38e^{-32t}\cos(2\pi 120t) + 0.2\cos(2\pi 1275t - 120°). \end{aligned} \quad (10)$$

Where $triang(2\pi f_0 t)$ represents a triangular wave of frequency, f_0. Each signal exhibits a different DC offset component, a triangular waveform out of phase by 120° with a fundamental frequency of $f_0 = 50$ Hz, a different exponential function, a damped cosine at 120 Hz, and a cosine at 1275 Hz with amplitude of 0.2, also phase-shifted by 120°.

The harmonic content of the signals is derived from the triangular waveforms whose harmonics occur at odd multiples of the fundamental frequency. The time step is $\Delta t = 10\ \mu s$, and the observation time is $T = 0.06$s. The implementation of the proposed methodology to estimate the harmonic content of the signals (10) for 1 (fundamental component), 50 and 1000 harmonics can now be described, along with the non-harmonic components. The value $N = 5$ poles is established, consisting of $N_h = 1$ harmonic (corresponding to one pair of complex conjugate poles), $N_n = 2$ poles plus 1 additional to approximate the test signals using only 1 harmonic (fundamental component) and some extra non-harmonic components, depending on whether VF converges to complex conjugate poles or purely real poles. The cut-off frequency for the frequency domain data is set to 100 Hz.

The behavior of the synthetic test signals and their approximations are shown in Fig. 3a. Both steady-state and transient-state responses show an acceptable approximation. The rational approximations of the NLT data for each signal through VF, along with its respective deviations using the absolute errors calculation, are shown in Fig. 3b. Additionally, Fig. 3c displays the absolute error in the time domain for the approximation of $f_1(t)$ including both harmonic and non-harmonic components. The estimated amplitude spectrum, including the DC-offset and phase spectrum, are shown in Fig. 4a and 4b, respectively. The proposed methodology accurately calculates the phases of the fundamental component of an electrical system. Fig. 4c illustrates the steady-state (fundamental and harmonic components) and the transient-state (non-harmonic components) responses.

Next, in accordance with the requirements of the IEEE 519 standard [13], a second approximation using 50 harmonics is carried out. The value $N = 131$ poles is established, consisting of $N_h = 50$ harmonics, $N_n = 30$ poles plus 1 additional pole to approximate the test signals using 100 complex conjugate poles (harmonics), with the remaining poles allocated to the non-harmonic components. The cut-off frequency for the frequency domain data is 2500 Hz. Figs. 5 and 6 present results similar to those in the previous case. In this case the TD approximation of the signals is more accurate, according to Fig. 5a and the absolute error shown in Fig. 5c. In this case, the cut-off frequency includes the frequency of the non-harmonic components in (10). Therefore, this estimation is more accurate, as shown in Fig. 5b. The amplitude spectrum and phase spectrum are shown in Fig. 6a and 6b, respectively, and Fig. 6c shows the steady-state and the transient-state responses. A clear separation of both responses is observed. To further verify the accuracy of the method in the presence of noise, the signals are contaminated with zero-mean Gaussian noise. A signal-to-noise-ratio (SNR) of 30 dB is used for each synthetic signal. The obtained results are shown in Figs. 7 and 8 where an accurate estimation of the components is observed.

Finally, the synthetic signals (10) are approximated using 1000 harmonics, which fall within the range of supraharmonics. The value is set at $N = 2031$ poles; that is, $N_h = 1000$ harmonics, $N_n = 30$ poles plus 1 additional. The cut-off frequency for the frequency domain data is 50,000 Hz. Figs. 9 and 10 show the same results as for the previous cases. This approximation demonstrates a lower error level.

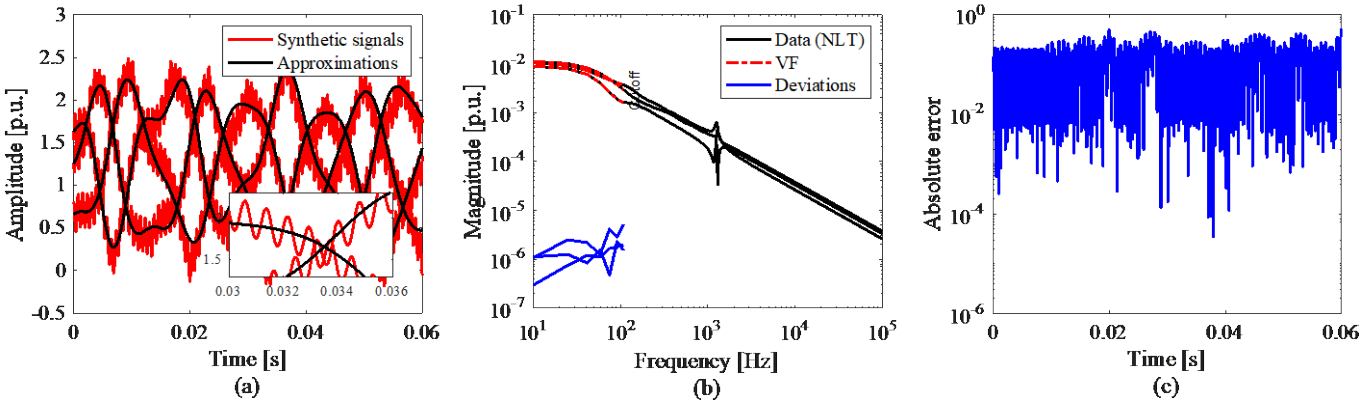

Fig.3. (a) Synthetic test signals and their approximations, (b) NLT data and fitting deviations, (c) Absolute error for the approximation in TD of $f_1(t)$.

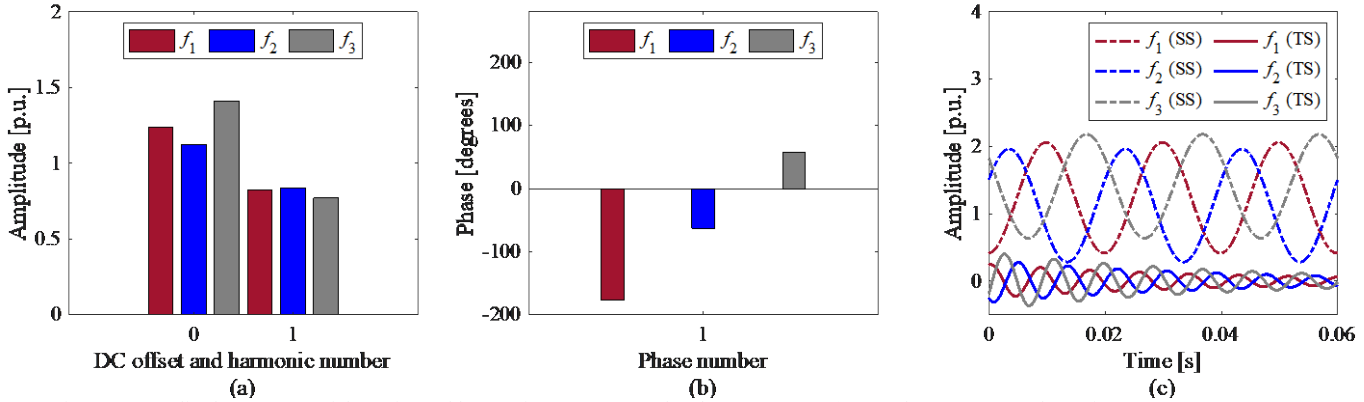

Fig.4. (a) Amplitude spectrum of the estimated harmonic components, (b) Phase spectrum, (c) Steady-state (SS) and transient-state (TS) responses.

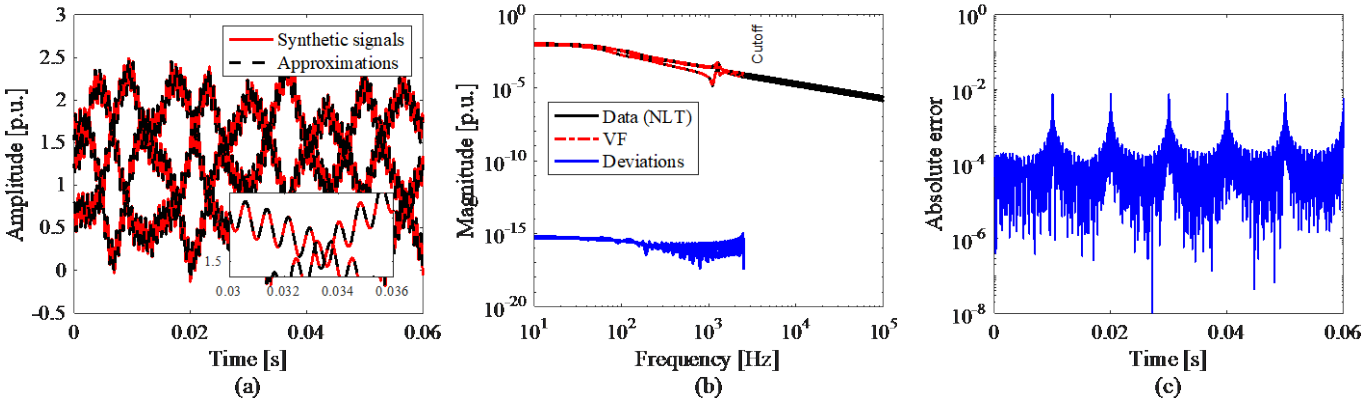

Fig.5. (a) Synthetic test signals and their approximations, (b) NLT data and fitting deviations, (c) Absolute error for the approximation in TD of $f_1(t)$.

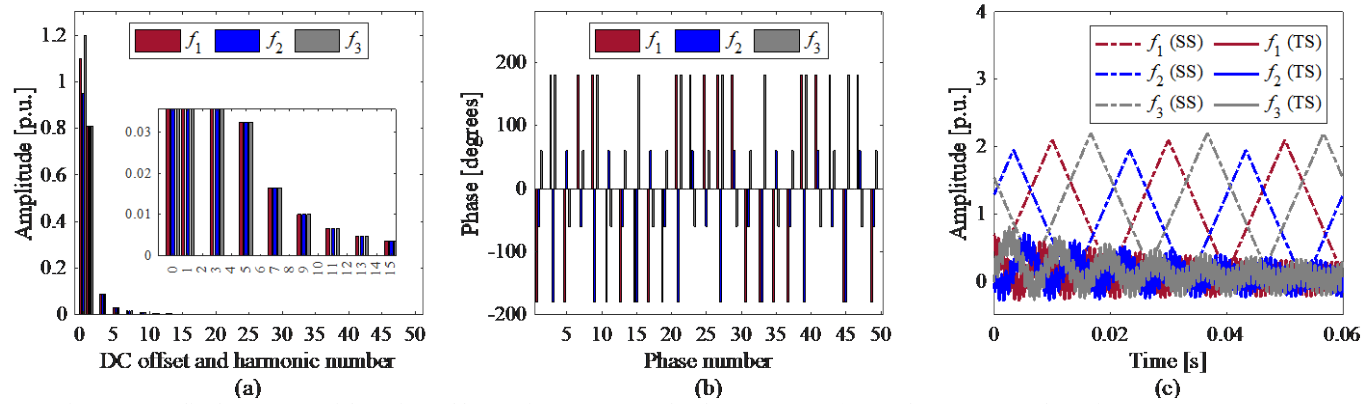

Fig.6. (a) Amplitude spectrum of the estimated harmonic components, (b) Phase spectrum, (c) Steady-state (SS) and transient-state (TS) responses.

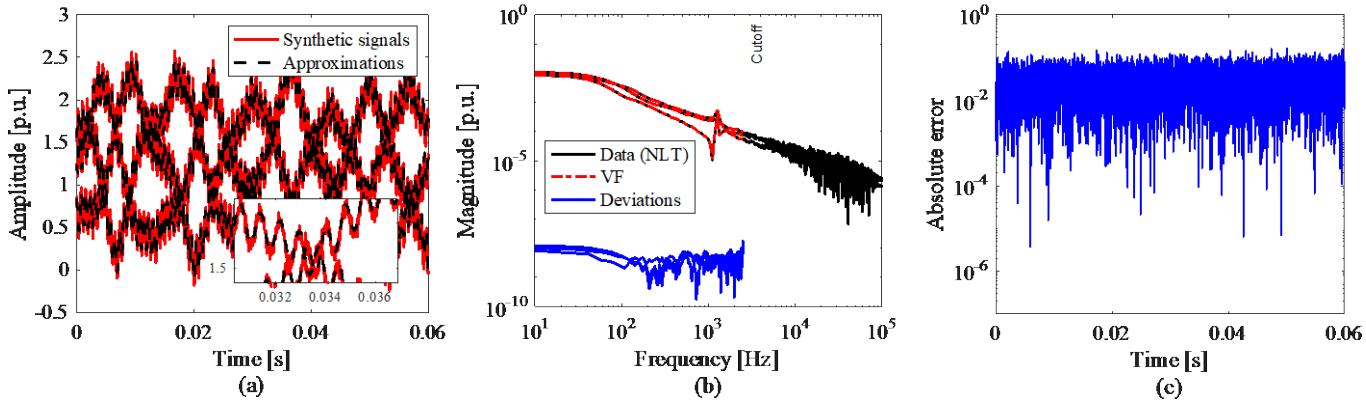

Fig.7. (a) Synthetic test signals and their approximations, (b) NLT data and fitting deviations, (c) Absolute error for the approximation in TD of $f_1(t)$.

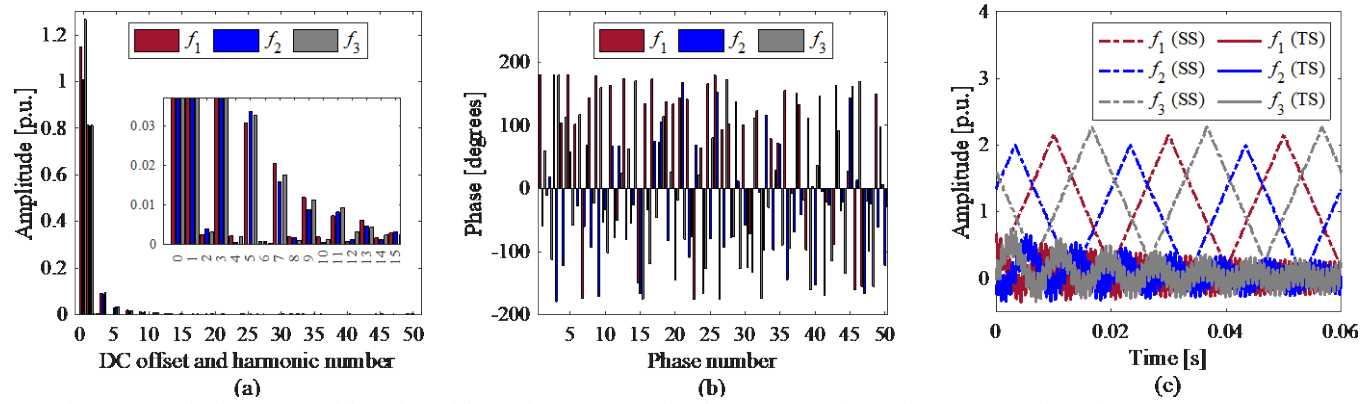

Fig.8. (a) Amplitude spectrum of the estimated harmonic components, (b) Phase spectrum, (c) Steady-state (SS) and transient-state (TS) responses.

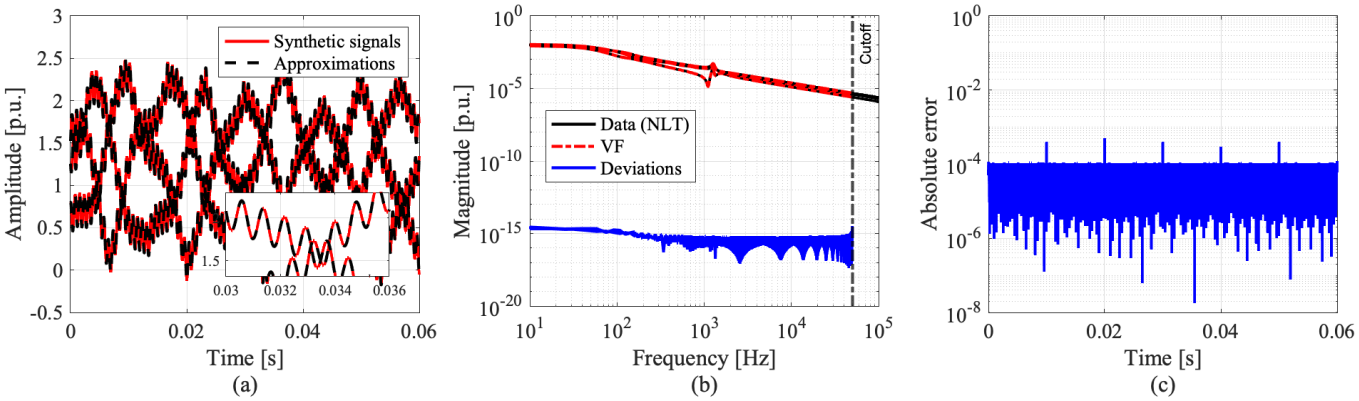

Fig.9. (a) Synthetic test signals and their approximations, (b) NLT data and fitting deviations, (c) Absolute error for the approximation in TD of $f_1(t)$.

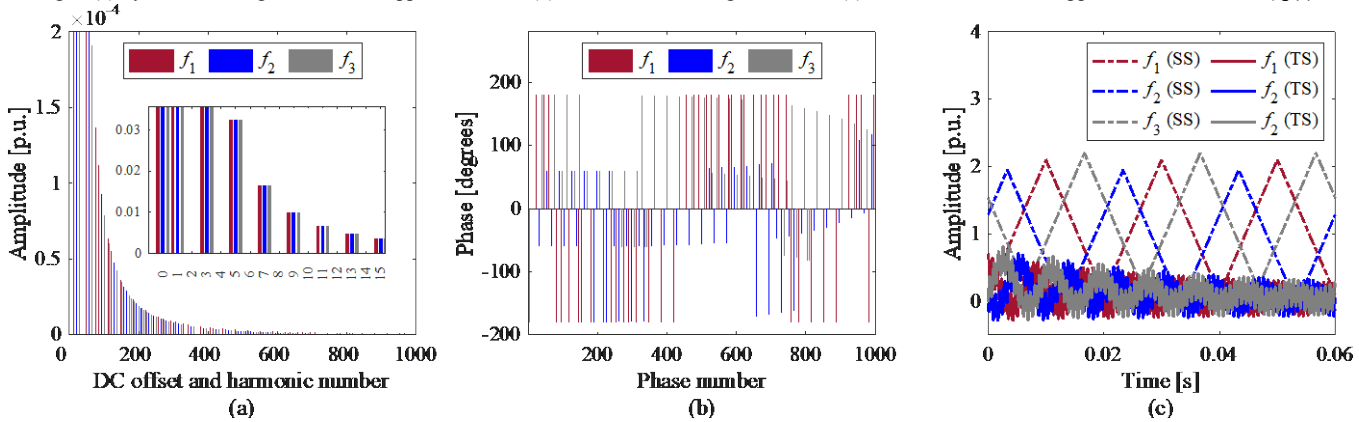

Fig.10. (a) Amplitude spectrum of the estimated harmonic components, (b) Phase spectrum, (c) Steady-state (SS) and transient-state (TS) responses.

B. Speed control of an induction motor using a three-phase space vector (SV) PWM technique.

This Simulink example demonstrates the open-loop speed control of an induction motor using the constant V/Hz principle and the space vector SV-PWM technique with a switching frequency of $f = 1980$ Hz [14].

The start-up currents of the stator are analyzed over a time window $T = 0.4$s with a base current of 18.725A and a constant speed reference. The time step is $\Delta t = 2$ μs. The component estimation is performed using 50 harmonics of the fundamental frequency $f_0 = 60$ Hz. The parameter set is $N = 131$; that is, $N_h = 50$, $N_n = 30$ poles, and 1 additional pole to approximate the current signals using 50 harmonics and the rest for the non-harmonic components. The cut-off frequency for the frequency domain data is 3000 Hz.

The behavior of the stator currents and their approximations are shown in Fig. 11a. The rational approximations of the NLT data for each current signal, along with their respective deviations calculated using absolute errors, are shown in Figure 11b. Additionally, Figure 11c illustrates the absolute error in the time domain (TD) for the approximation of phase A, including harmonics and non-harmonics. The estimated amplitude and phase spectra are shown in Figs. 12a and 12b, respectively; Fig. 12c separately displays the steady-state (harmonic components) and the transient-state (non-harmonic components) responses. The results indicate that harmonic and non-harmonic components have been estimated with a high degree of accuracy.

IV. Discussion

The proposed methodology effectively calculates the harmonic and non-harmonic components of one or more signals by incorporating a known harmonic base.

To demonstrate the contribution of this base and the effect of the proposed iterative refinement, a triangular signal will be employed, with an observation time of $T = 0.08$ s, a time step of $\Delta t = 10$ μs, and a fundamental frequency of $f_0 = 60$ Hz, whose harmonics are present in odd multiples of the fundamental frequency [15].

Three tests are conducted to calculate 200 harmonics, including even and odd harmonics: 1) using VF in the NLT data of the signal, 2) using VF in the NLT data of the signal with the added harmonic base, and 3) using VF in the NLT data of the signal with the added harmonic base and iterative refinement (proposed methodology).

Fig.13a shows the pole diagram obtained from the first test. Some poles converge to the odd harmonics but not to the even ones, which is to be expected due to the harmonic content of the signal. Fig. 13b presents the pole diagram obtained from the second test. The poles are closer to the added harmonic base but still exhibit inaccuracies.

Finally, Fig. 13c displays the pole diagram obtained using the proposed methodology. The poles align with the 200 harmonics, forcing VF to converge to the added base. This allows accurately calculating the signal components.

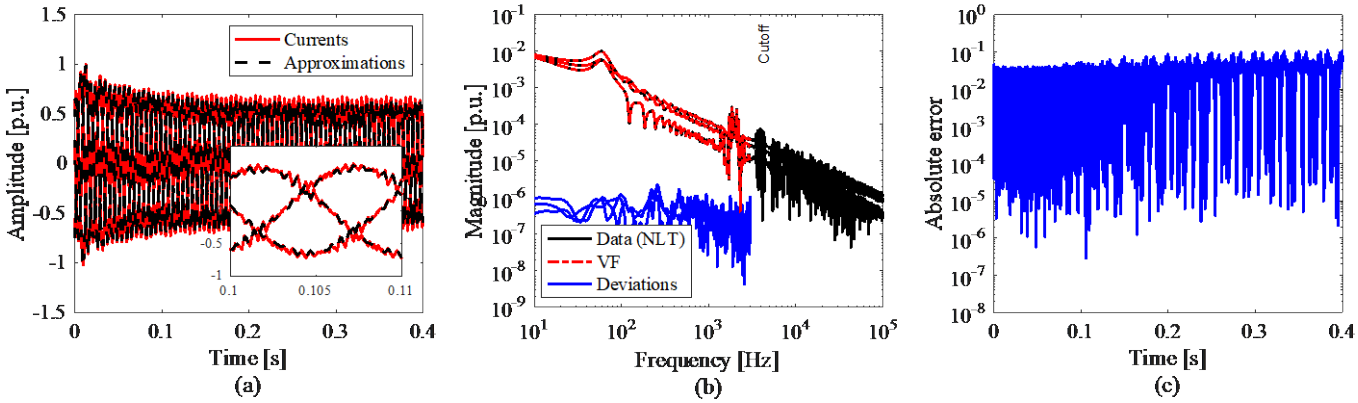

Fig.11 (a) Stator currents and their approximations, (b) NLT data and fitting deviations, (c) Absolute error for the approximation in TD for phase A.

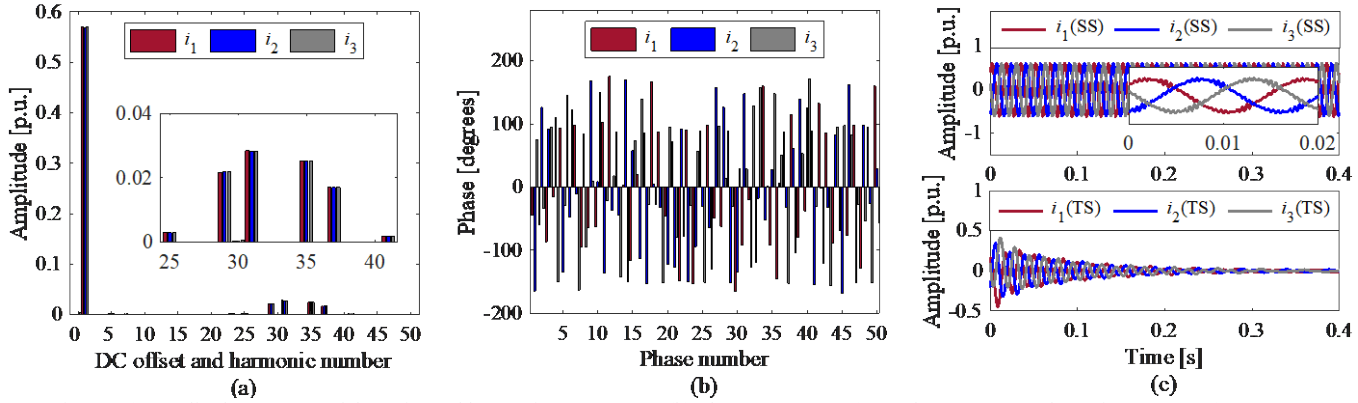

Fig.12. (a) Amplitude spectrum of the estimated harmonic components, (b) Phase spectrum, (c) Steady-state (SS) and transient-state (TS) responses.

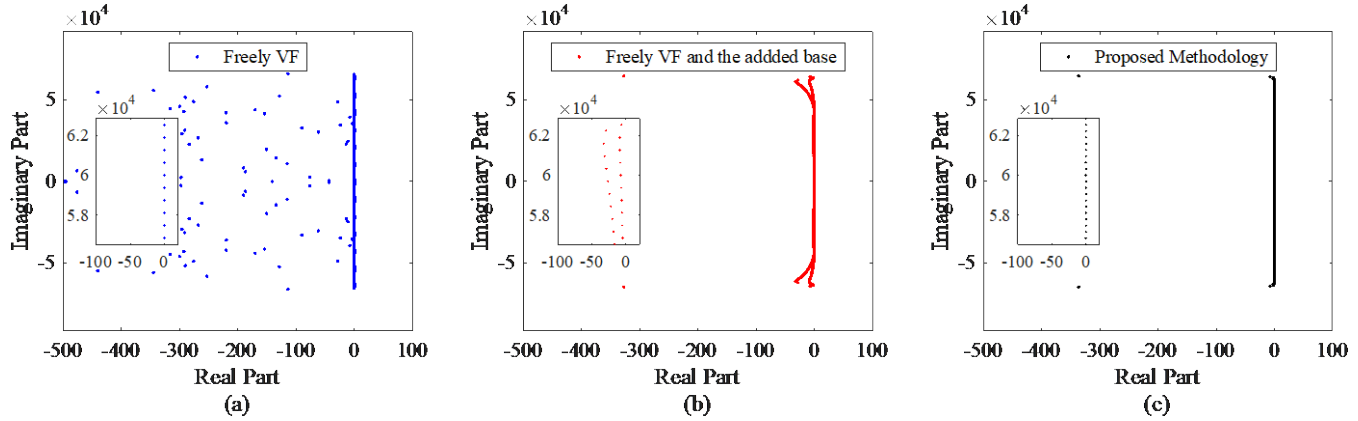

Fig.13. Rational approximation using VF in, (a) the NLT data of the signal, (b) the NLT data of the signal + the added base (c) the NLT data of the signal + the added base + iterative refinement.

V. CONCLUSIONS

A precise methodology is presented for the estimation of harmonic components and non-harmonic components (subharmonics, interharmonics, and DC offset) in electrical systems.

This methodology combines the NLT and VF methods with an approach that allows VF to converge to a harmonic base. The main conclusions are as follows:

1) This methodology can simultaneously estimate the amplitude and phase of each harmonic component and the amplitude, damping, frequency, and phase of each non-harmonic component (subharmonic or interharmonic) and the DC offset contained in a signal or a signal set including noisy signals.

2) Parameter identification achieves high accuracy due to the error level achieved by both the NLT and the conventional VF methods.

3) This methodology can determine the phases of the fundamental component of a multiphase system, even in the presence of harmonics and non-harmonics.

4) The examples validate the strong performance of the proposed metodology for a wide frequency range.

5) This methodology is applicable in previously established frequency bands to carry out studies in only ranges of interest.

VI. References

[1] Á. Espín Delgado, "Propagation of Supraharmonics in Low-Voltage Networks," PhD dissertation, Luleå University of Technology, Luleå, 2022.

[2] Lu, J., Zhao, X., and Yamada, S., *Harmonic Balance Finite Element Method: Applications in Nonlinear Electromagnetics and Power Systems*, New York: Wiley, 2016.

[3] S. T. Y. Alfalahi et al., "Supraharmonics in Power Grid: Identification, Standards, and Measurement Techniques," *in IEEE Access*, vol. 9, pp. 103677-103690, 2021.

[4] Á. Espín-Delgado, S. Rönnberg, S. S. Letha, M. Bollen, "Diagnosis of supraharmonics-related problems based on the effects on electrical equipment," *Electric Power Systems Research*, vol. 195, 2021.

[5] K. Sheshyekani, G. Fallahi, M. Hamzeh and M. Kheradmandi, "A General Noise-Resilient Technique Based on the Matrix Pencil Method for the Assessment of Harmonics and Interharmonics in Power Systems," *in IEEE Transactions on Power Delivery*, vol. 32, no. 5, pp. 2179-2188, Oct. 2017.

[6] S. K. Jain, S.N. Singh, "Harmonics estimation in emerging power system: Key issues and challenges," *Electric Power Systems Research*, vol. 81, no. 9, pp. 1754-1766, 2011.

[7] B. Gustavsen and A. Semlyen, "Rational approximation of frequency domain responses by vector fitting," *in IEEE Transactions on Power Delivery*, vol. 14, no. 3, pp. 1052-1061, July 1999.

[8] E.S. Bañuelos-Cabral, J.J. Nuño-Ayón, B. Gustavsen, J.A. Gutiérrez-Robles, V.A. Galván-Sánchez, J. Sotelo-Castañón, J.L. García-Sánchez, "Spectral fitting approach to estimate electromechanical oscillation modes and mode shapes by using vector fitting," *Electric Power Systems Research*, vol. 176, 2019.

[9] E.S. Bañuelos-Cabral, J.A. Gutiérrez-Robles, J.J. Nuño-Ayón, J. Sotelo-Castañón, J.L. Naredo, "Extended vector fitting for subharmonics, harmonics, interharmonics, and supraharmonics estimation in electrical systems," *Electric Power Systems Research*, vol. 224, 2023.

[10] L.M Wedepohl and S.E.T. Mohamed, "Transient analysis of multiconductor transmission lines with special reference to nonlinear problems," *in Proceedings of the Institution of Electrical Engineers*, vol. 117, no. 5, May 1970.

[11] P. Moreno, *Análisis de transitorios con la transformada numérica de Laplace*, second ed., Editorial Académica Española, España, 2012.

[12] P. Moreno and A. Ramirez, "Implementation of the Numerical Laplace Transform: A Review," *in IEEE Transactions on Power Delivery*, vol. 23, no. 4, pp. 2599-2609, Oct. 2008.

[13] "IEEE Standard for Harmonic Control in Electric Power Systems," *in IEEE Std 519-2022* (Revision of IEEE Std 519-2014), vol., no., pp.1-31, 5 Aug. 2022.

[14] Documentation, *Simulation and model-based design*, MathWorks, 2024b. Retrieved from: https://la.mathworks.com/help/sps/ug/three-phase-sv-pwm-converter.html

[15] B.P. Lathi, Principles of linear systems and signals, second ed., Oxford university press, United Kingdom, 2009.